Superlattices and Microstructures 34 (2003) 301–310

Superlattices and Microstructures

www.elsevier.com/locate/superlattices

Two-dimensional electrical characterization of ultrashallow source/drain extensions for nanoscale MOSFETs

U. Singisetti[a,*], M.R. McCartney[b], J. Li[b], P.S. Chakraborty[a], S.M. Goodnick[a], M.N. Kozicki[a], T.J. Thornton[a]

[a] *Center for Solid State Electronics Research, Arizona State University, Tempe, AZ 85287-6206, USA*
[b] *Center for Solid State Science, Arizona State University, Tempe, AZ 85287-1704, USA*

Available online 20 April 2004

Abstract

State-of-the-art semiconductor devices require accurate control of the full two-dimensional dopant distribution. In this work, we report results obtained on 2D electrical characterization of ultra shallow junctions in Si using off axis electron holography to study two-dimensional effects on diffusion. In particular, the effect of a nitride diffusion mask on lateral diffusion of phosphorous is discussed. Retardation of lateral diffusion of P under the nitride diffusion mask is observed and compared to the lateral diffusion of P under an oxide diffusion mask. The ultra shallow junctions for the study were fabricated by a rapid thermal diffusion process from heavily P doped spin-on-dopants into a heavily B doped Si substrate. These shallow junctions are needed for fabricating source/drain extensions in nanoscale MOSFETs. One-dimensional electrical characterization of the junction was carried out to determine the electrical junction depth and compared to the metallurgical junction depth from SIMS analysis.

Keywords: Electron holography; Ultra shallow junctions; Dopant activation; Rapid thermal diffusion; Space charge region; Lateral diffusion; 2D characterization; Lateral abruptness; Phosphorous diffusion; Nitride spacer

1. Introduction

Continued scaling of CMOS beyond the 100 nm node demands accurate control of the complete two-dimensional (2D) distribution of dopants in ultra shallow junctions (USJ)

* Corresponding author. Tel.: +1-480-965-4096; fax: +1-480-965-3836.
E-mail address: uttam@asu.edu (U. Singisetti).

0749-6036/$ - see front matter © 2004 Elsevier Ltd. All rights reserved.
doi:10.1016/j.spmi.2004.03.020

for source/drain extensions. The International Technology Roadmap for Semiconductors (ITRS/Roadmap) identifies the key challenges for source/drain extensions technology [1]. The Roadmap predicts that source/drain extensions will require a junction depth less than 40 nm with high depth and lateral abruptness, and low sheet resistance. The Roadmap emphasizes the development of high quality 2D metrology with nanoscale resolution.

Off axis electron holography (EH) is used in this investigation to perform 2D electrical characterization of USJs for source/drain extensions. This technique has been successfully used for mapping electrostatic potential in semiconductor devices with nanometer spatial resolution [2–7]. Off axis EH is a transmission electron microscope (TEM) technique that provides quantitative information about the phase shift of the electron wave front due to the interaction with the electrostatic potential of the specimen. As the phase shift is associated with the electrostatic potential of the medium, it gives the potential distribution in the space charge region (SCR) of USJ. In EH, the interference pattern of a high energy electron wave front scattered by an electron transparent specimen with a coherent reference electron wave front is reconstructed to derive the phase and amplitude information of the electron wave front through the specimen. The reconstructed phase image contains the quantitative information of the electrostatic potential in the sample. Digital recording of the hologram with a slow scan charge coupled device (CCD) camera facilitates higher sensitivity and digital processing has improved quantitative holography [8–10].

In this investigation, EH is used to study the 2D diffusion of phosphorous in ultra shallow junctions in Si, and the influence of diffusion mask on the lateral diffusion of phosphorous. The electrical junction depth (EJD) is estimated from the potential profile derived from the phase image and Poisson's equation, and compared with EJD, electric field and total charge from the simulation of the SIMS profile shown in Fig. 1.

2. Sample preparation and experimental details

A spin-on-dopant (SOD) and rapid thermal diffusion (RTD) process was used to fabricate ultra shallow junctions for this study. This technology for USJ was found to be suitable for source/drain extensions in sub 100 nm MOSFETs [11]. Phosphorous in the SOD was incorporated into heavily (Boron) doped p-type Si substrate using RTD at 850 °C. 200 nm of low-pressure chemical vapor deposition (LPCVD) silicon nitride was deposited on a heavily P-doped [100] Si substrate. 180 nm of Al was deposited and patterned by lift-off process to act as etch mask for the nitride. Reactive ion etching was used to open a diffusion window in the nitride film, Al is then removed by etching in a dilute acid. The P doped SOD was spun, baked and treated with a RTD process to form an n^+p ultra shallow junction in the diffusion window.

Two samples were fabricated using this RTD process at 850 °C, one given a low thermal budget and the other a slightly higher thermal budget. The SOD after diffusion was removed by etching in a HF solution for further analysis. SIMS was done on both junctions in a region completely unmasked by nitride. 100 nm of Cr was deposited on the sample for EH investigation for protection of the surface during TEM sample preparation.

A wedge polishing technique was used to make cross-sectional TEM samples resulting in a 2° wedge in the specimen [11–13]. Further thinning of the sample was done by low

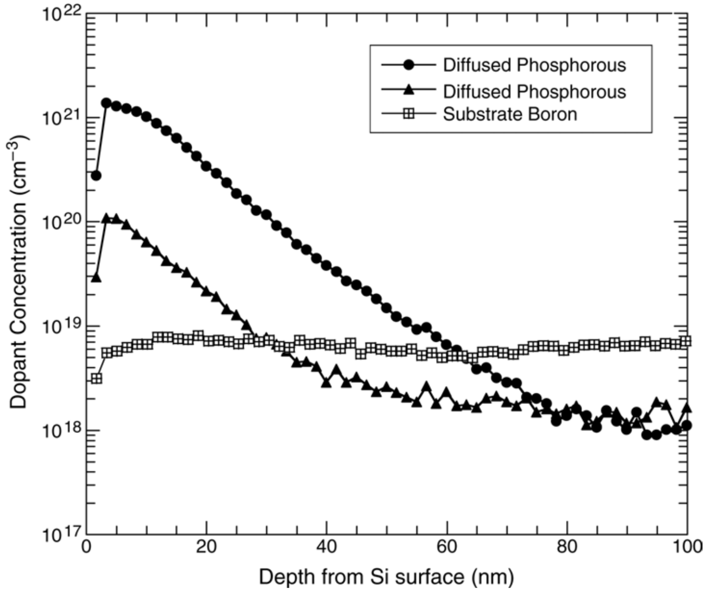

Fig. 1. SIMS profiles of dopants in the samples fabricated using RTD for electron holography. The MJD for the two junctions are 30 nm and 65 nm as seen above.

angle (∼6°) low energy (20 keV) ion milling to get the cross-section thickness between 200–300 nm for EH. This thickness range helps in getting reliable phase shifts in the hologram due to the potential variation in the SCR of the USJ.

Electron holograms were acquired using a 200 keV Philips CM200-FEG TEM equipped with a special Lorentz lens [14] and a 1024 × 1024 Gatan 794 CCD camera. The Lorentz lens was used to optimize the field of view. The samples were tilted away from the [110] zone axis to the minimal diffraction condition, keeping the junction 1°–2° from the edge on. Digital holograms were reconstructed from the interference of the electron wave front through the specimen and the electron wave front through vacuum that was present in the field of view. Reconstructed amplitude images were used to derive the corresponding 2D thickness image using 85 nm as the mean free path (λ_i) for Si inelastic scattering [15]. A 1D Poisson solver [16] was used to simulate potential profile, electric field and total charge distribution of the junctions with the dopant distribution as measured by SIMS.

3. Results and analysis

A Cs^+ primary ion SIMS analysis was done on the shallow junctions to determine the 1D B and P concentration profile. The metallurgical junction depth (MJD) is defined as the depth from surface at which the concentration of boron atoms in the substrate is equal to the concentration of phosphorous incorporated by RTD. The substrate boron concentration is $\sim 4 \times 10^{18}$ as measured by SIMS. The MJD as observed in the SIMS profile of B and P in Fig. 1 is 30 nm and 65 nm respectively for the two junctions fabricated.

The reconstructed phase images of the junctions from the two samples are shown in Figs. 2 and 3(a). The phase enhancement due to the diffused n^+ region over the p-type substrate [12, 13] appears as the bright region in the phase image. In both the phase images we see a brighter region at the surface that indicates the presence of an n^+p junction. The dark lines are depth at which half the total variation of the electrostatic potential in SCR occurs. The line shows the approximate electrical junction depth. The phase images are scaled into potential maps using

$$V(x, y) = \frac{\phi(x, y)}{C_E \cdot t(x, y)} - V_0, \tag{1}$$

where $\phi(x, y)$ is the phase shift relative to vacuum, C_E is an interaction constant depending on the acceleration voltage (0.00728 rad V^{-1} nm^{-1} at 200 keV), and V_0 is taken as the mean inner potential of Si [17]. $V(x, y)$ and $t(x, y)$ are the spatially varying 2D potential and thickness mapping respectively across the sample.

1D analysis of the 30 nm MJD junction was carried out in a similar way as detailed in previous work [12, 13]. Fig. 2(b) shows the potential drop of ∼1.25 V from the silicon surface to the substrate, as is expected from a highly doped degenerate junction [12, 13]. The electric field and total charge distribution associated with the SCR of the junction were obtained by successive differentiation of the 1D potential profile from EH. This numerical differentiation process is inherently noisy, particularly in the charge density, which is derived from the second order derivative of the potential profile. So a polynomial fit of the potential profile in Fig. 2(b) is used to derive the electric field and total charge distribution. Fig. 4(a) shows the extracted electric field, charge density for the 30 nm MJD specimen. In comparison, Fig. 4(b) shows the simulated electric field and total charge distribution calculated from the Poisson Solver [16] using the measured SIMS profile of Fig. 1. The electrical junction depth (EJD) is defined to be the depth from surface at which the maximum of the electric field occurs or the total charge density associated with the SCR of the USJ goes to zero. The EJD from the EH is found to be ∼25 nm as seen in Fig. 4(a), which matches closely with the MJD from the SIMS analysis. The EJD as determined from the simulation of the SIMS profile is ∼26 nm. Better fits for the simulated quantities with experimental values were obtained by assuming activation of 50% for the diffused atoms. The lower activation values estimated and the difference in the simulated charge profile from SIMS data and the charge profile from EH can be due to a combination of reasons. The SIMS data gives an upper limit on the junction depth due to “knock-on” effect. A Cs^+ primary ion SIMS measurement carried out on a delta layer of P showed a significant amount of “knock-on” tail to affect the SIMS data for the 30 nm MJD sample. Higher estimation of the activation could be possible if the “knock-on” effect was taken into account. Moreover the comparison between EH and simulation from SIMS is limited by the spatial resolution limit of the holographic data, which is limited to 5 nm in this analysis and depth resolution limits of SIMS. Similar 1D analysis of the 65 nm junction gave an EJD of ∼64 nm from the EH data. And an EJD of ∼64 nm was obtained from the simulation of the SIMS profile assuming 100% activation.

A very significant feature is revealed in the phase images in Figs. 2 and 3(a), the lateral diffusion is less than 5 nm, as seen by the brightness contrast of the phase image. The lateral diffusion stops very near the nitride mask edge. In comparison, the lateral diffusion

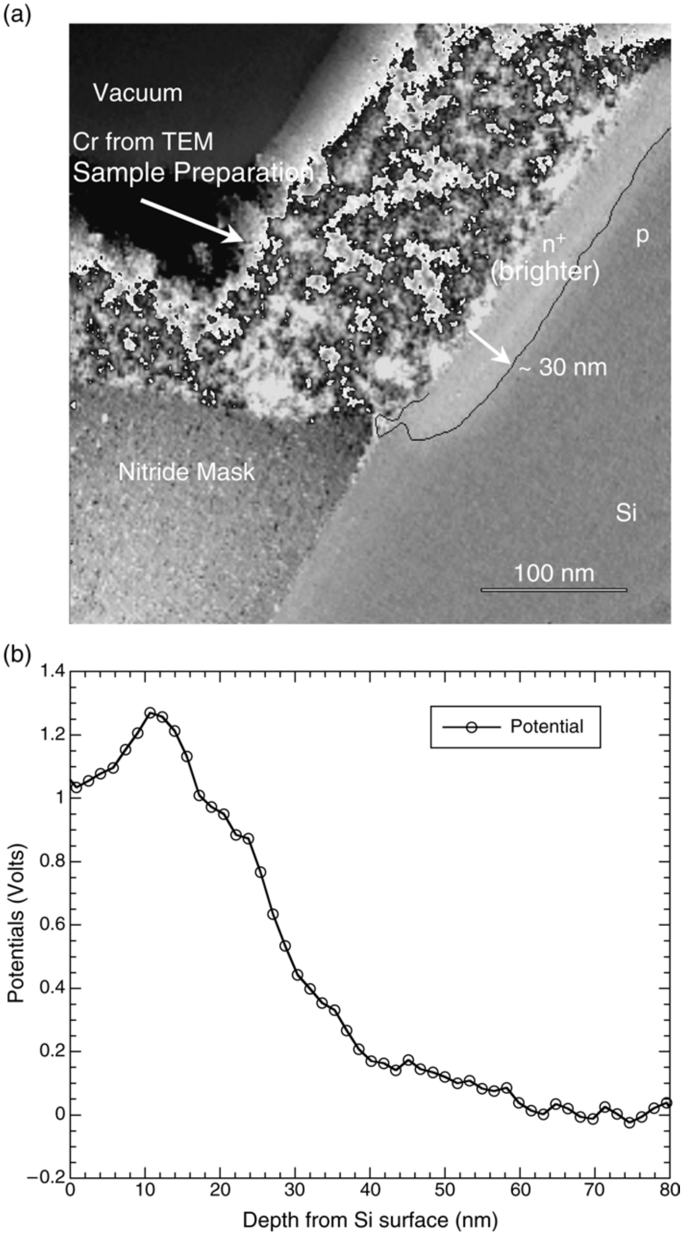

Fig. 2. (a) Potential image from the reconstructed phase image of a region of the 30 nm MJD sample showing the bright region as a contrast due to the USJ formation. The dark contour line is the point of half the total variation of the electrostatic potential within SCR. (b) 1D potential profile calculated from the phase and thickness line scans away from the mask edge.

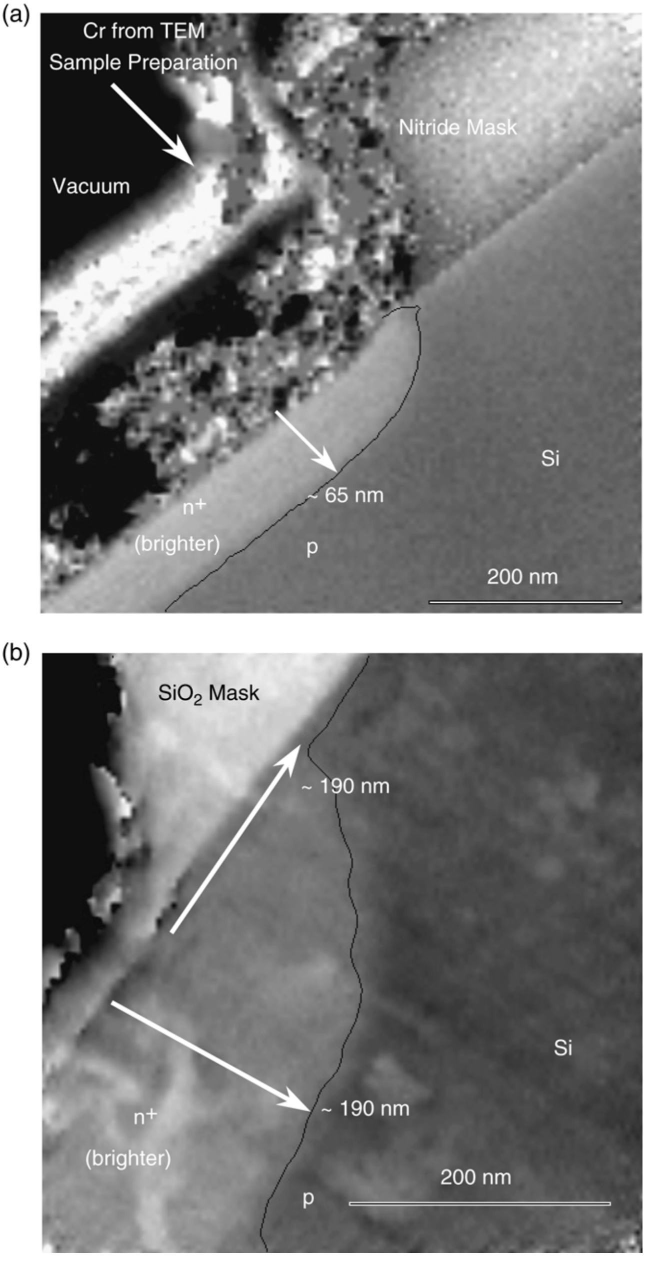

Fig. 3. (a) Potential image from the reconstructed phase map of a region of the 65 nm MJD sample showing the bright region as a contrast due to the USJ formation. (b) Potential image from the reconstructed phase image of the sample with oxide diffusion mask, the bright region indicating the junction formation. The dark contour lines are the points of half the total electrostatic potential variation across the SCR.

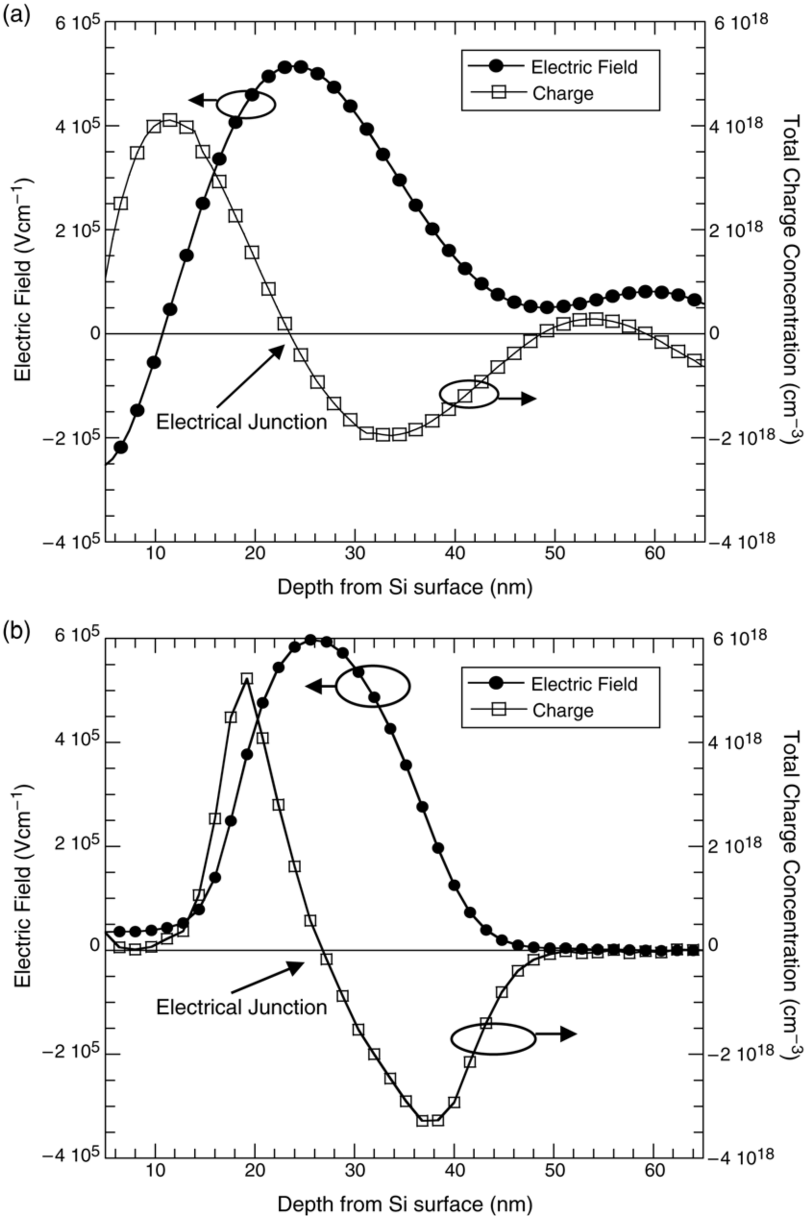

Fig. 4. (a) 1D electric field and total charge distribution calculated from the potential profile in Fig. 2(b). (b) 1D electric field and total charge distribution from the simulation of the SIMS profile of 30 nm MJD junction.

shown in the phase image of Fig. 3(b) with oxide as diffusion mask, is comparable with the vertical diffusion. The observed anisotropic diffusion of P can possibly be explained by the effect of stress at the nitride film edge. LPCVD silicon nitride films are found to be under high intrinsic tensile stress [18, 19]. Under this LPCVD silicon nitride film edge, the Si substrate is under high anisotropic, compressive stress [18, 20]. The stresses in the Si substrate are known to affect the diffusion process depending on the mechanism of the diffusion. It has been observed that the diffusion of P in Si, which is an interstitial mediated process, is retarded under a silicon nitride film [21]. In contrast, there is enhancement of the diffusion Sb [21], which is a vacancy mediated process. Stress is known to introduce anisotropy in the diffusion process [22–24]. Enhanced lateral diffusion of Sb compared to vertical diffusion has been observed and measured in Si substrate under nitride spacers using scanning spreading resistance microscopy (SSRM) [24]. In this case the LPCVD nitride film induces anisotropic compressive stresses in Si near the film edge. This higher lateral stress compared to the vertical stress [20] retards the interstitial mediated diffusion of P in the lateral direction. This effect can be clearly seen in the phase images of both the junctions. In contrast, the phase image in Fig. 3(b) with oxide as a diffusion mask shows a lateral diffusion that is about the same as vertical diffusion. This effect can be accounted for by the fact that thermally grown oxide does not exhibit significant intrinsic stresses associated with it [18, 19], which means it does not limit the lateral diffusion of P. As the diffusion coefficient of P in oxide is higher than in nitride, it diffuses through the gradual edge of the oxide mask. These two factors lead to a higher lateral diffusion seen in the case of the junction with oxide mask in Fig. 3. The junction with oxide diffusion mask was fabricated using the same technique used for the nitride diffusion mask and electrically characterized similar to the way here in a previous study [13].

4. Summary

We have observed retardation of lateral diffusion of P under a nitride mask in USJs using EH, which has a possible explanation associated with the stresses in the substrate due to the diffusion mask. EH was successfully used to electrically characterize USJs. The fabricated USJ's in this study with high lateral abruptness are highly desirable for source extensions in nanoscale MOSFETs. The high lateral abruptness in source extension leads to higher source injection velocity and higher resulting drive current. As devices get smaller into the sub 100 nm regime, the effects of lateral diffusion and stress become significant. Electron holography with its nanoscale resolution has emerged as an important tool to realize further insight into the processing technology.

Acknowledgements

This work was supported by the Office of Naval Research MURI program and by the Semiconductor Research Corporation under the grant SRC#2001-MJ-942. The authors would like to thank the Center for High Resolution Electron Microscopy, and K. Franzerb of the SIMS facility at Arizona State University for assistance. The authors would like to acknowledge the referee for the SIMS data interpretation and would like to thank Dr. P. Williams and Dr. R. Hervig for informative discussions.

References

[1] International Technology Roadmap for Semiconductors: Front End Processes, Semiconductor Industry Association, San Jose, CA, 2001, Available http://public.itrs.net/Files/2001ITRS/.

[2] M.R. McCartney, D.J. Smith, R. Hull, J.C. Bean, E. Völkl, B. Frost, Direct observation of potential distribution across Si/Si p–n junctions using off-axis electron holography, Applied Physics Letters 65 (20) (1994) 2603–2605.

[3] W.D. Rau, F.H. Baumann, H.H. Vuong, B. Heinemann, W. Höppner, C.S. Rafferty, H. Rücker, P. Schwander, A. Ourmazd, Two-dimensional dopant profiling of deep submicron MOS devices by electron holography, International Electron Devices Meeting Tech. Digest (1998) 713–716.

[4] W.D. Rau, P. Schwander, F.H. Baumann, W. Höppner, A. Ourmazd, Two-dimensional mapping of the electrostatic potential in transistors by electron holography, Physical Review Letters 82 (12) (1999) 2614–2617.

[5] M.A. Gribelyuk, M.R. McCartney, J. Li, C.S. Murthy, P. Ronsheim, B. Doris, J.S. McMurray, S. Hegde, D.J. Smith, Mapping of electrostatic potential in deep submicron CMOS devices by electron holography, Physical Review Letters 89 (2) (2002) 025502(1–4).

[6] M.R. McCartney, M.A. Gribelyuk, J. Li, P. Ronsheim, J.S. McMurray, D.J. Smith, Quantitative analysis of one-dimensional dopant profile by electron holography, Applied Physics Letters 80 (17) (2002) 3213–3215.

[7] A.C. Twichett, R.E. Dunin-Borkowski, P.A. Midgley, Quantitative electron holography of biased semiconductor devices, Physical Review Letters 88 (23) (2002) 238302(1–4).

[8] L. Reimer, Transmission Electron Microscopy, Springer Verlag, Berlin, 1989.

[9] A. Tonomura, L.F. Allard, G. Pozzi, D.C. Joy, Y.A. Ono (Eds.), Electron Holography, North-Holland, Elsevier, 1995.

[10] D.J. Smith, W.J. de Ruijter, J.K. Weiss, M.R. McCartney, Quantitative electron holography, in: E. Voelkl, L. Allard, D.C. Joy (Eds.), Introduction to Electron Holography, Plenum, New York, 1999 (Chapter 5).

[11] C. Gopalan, P.S. Chakraborty, J. Yang, T. Kim, Z. Wu, M.R. McCartney, S.M. Goodnick, M.N. Kozicki, T.J. Thornton, Shallow source/drain extensions for deep submicron MOSFETs using spin-on-dopants, IEEE Transactions on Electron Devices 50 (2003) 1277–1283.

[12] P.S. Chakraborty, M.R. McCartney, J. Li, C. Gopalan, M. Gilbert, S.M. Goodnick, T.J. Thornton, M.N. Kozicki, Shallow source/drain extensions for deep submicron MOSFETs using spin-on-dopants, IEEE Transactions on Nanotechnology 2 (2003) 102–109.

[13] P.S. Chakraborty, M.R. McCartney, J. Li, C. Gopalan, U. Singisetti, S.M. Goodnick, T.J. Thornton, M.N. Kozicki, Electron holographic characterization of nanoscale charge distributions for ultra shallow PN junctions in Si, Physica E 19 (2003) 167–172.

[14] M.R. McCartney, D.J. Smith, R.F.C. Farrow, R.F. Marks, Off-axis electron holography of epitaxial FePt films, Journal of Applied Physics 82 (1997) 2461–2465.

[15] M.R. McCartney, M. Gajdardziska-Josifovska, Absolute measurement of normalized thickness, t/λ_i, from off-axis electron holography, Ultramicroscopy 53 (1994) 283–289.

[16] I.-H. Tan, G.L. Snider, L.D. Chang, E.L. Hu, A self-consistent solution of Schrödinger-Poisson equations using a nonuniform mesh, Journal of Applied Physics 68 (8) (1990) 4071–4073, http://www.nd.edu/~gsnider/.

[17] M. Gajdardziska-Josifovska, M.R. McCartney, W.J. de Ruijter, D.J. Smith, J.K Weiss, J.M. Zuo, Accurate measurement of mean inner potential of crystal wedges using digital electron holograms, Ultramicroscopy 50 (1993) 285–299.

[18] S.M. Hu, Stress-related problems in silicon technology, Journal of Applied Physics 70 (6) (1991) R53–R79.

[19] S.M. Hu, Film-edge-induced stress in silicon substrates, Applied Physics Letters 32 (1) (1978) 5–7.

[20] P. Eyben, N. Duhayon, C. Suter, I. De Wolf, R. Rooyackers, T. Clarysse, W. Vandervorst, G. Badenes, SSRM and SCM observation of enhanced lateral As- and BF2-diffusion induced by nitride spacers, Materials Research Society Symposium 610 (2000) B2.2.1–B2.2.12.

[21] S.T. Ahn, H.W. Kennel, J.D. Plummer, W.A. Tiller, Film stress-related vacancy supersaturation in silicon under low-pressure chemical vapor deposited silicon nitride films, Journal of Applied Physics 64 (10) (1988) 4914–4919.

[22] P.H. Dederichs, K. Schroder, Anisotropic diffusion in stress fields, Physical Review B 17 (6) (1978) 2524–2536.

[23] M.S. Daw, W. Windl, N.N. Carlson, M. Laudon, M.P. Masquelier, Effect of stress on dopant and defect diffusion in Si: a general treatment, Physical Review B 64 (4) (2001) 045205(1–10).
[24] P. Eyben, N. Duhayon, C. Suter, I. De Wolf, R. Rooyackers, T. Clarysse, W. Vandervorst, G. Badenes, SSRM and SCM observation of modified lateral diffusion of As, BF2 and Sb induced by nitride spacers, Materials Research Society Symposium 669 (2001) J2.2.1–J2.2.6.